

Courtesy of CRC Press/Taylor & Francis Group

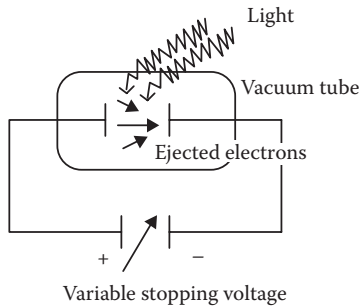


Figure 2.1 Schematic experimental setup for the photoelectric effect.

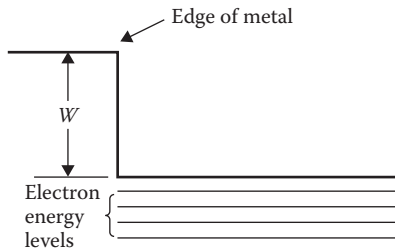


Figure 2.2 Schematic illustration of the work function, W , seen by electrons at the edge of a metal.

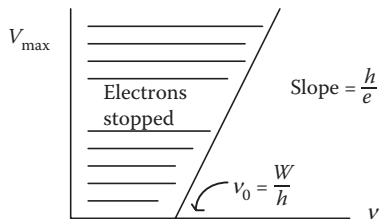


Figure 2.3 Relationship between V_{\max} and frequency, ν , for the photoelectric effect.

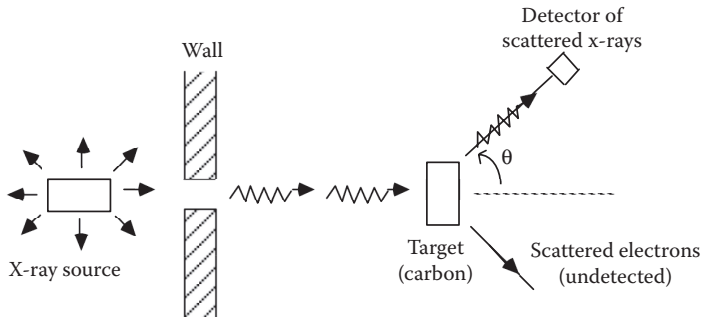


Figure 2.4 Schematic representation of the Compton experiment.

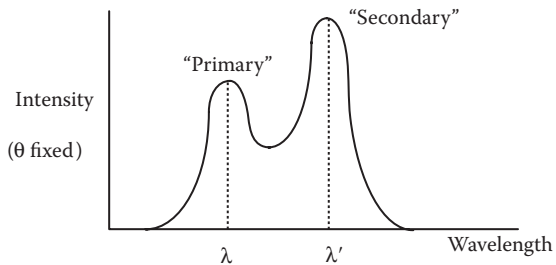


Figure 2.5 The two-peak result for intensity versus wavelength from the scattering of X-rays from electrons.

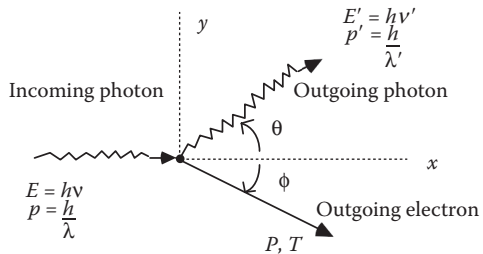


Figure 2.6 Kinematic diagram for the Compton effect. θ is the scattering angle for the X-ray.

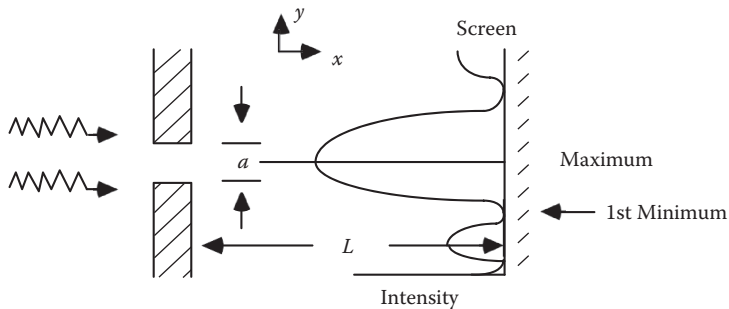


Figure 2.7 Schematic representation of a diffraction intensity pattern arising from a single slit.

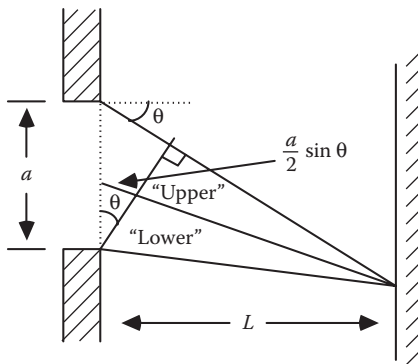


Figure 2.8 Geometry associated with locating the angular position of the first diffraction minimum from a single slit.

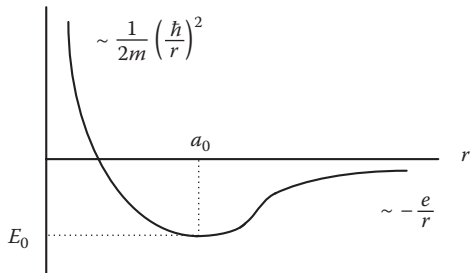


Figure 2.9 Effective ground state energy of hydrogen from the uncertainty principle.

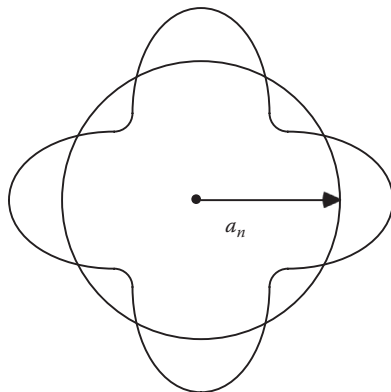


Figure 2.10 Schematic representation of the phase of an electron in a circular orbit around a proton.

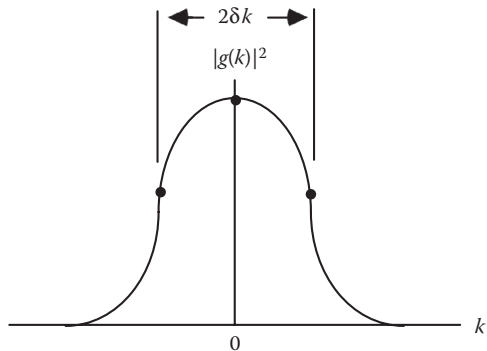


Figure 2.11 A function, $g(k)$, whose absolute square, $|g(k)|^2$, is peaked near the origin in k -space with an approximate full width of $2\delta k$.

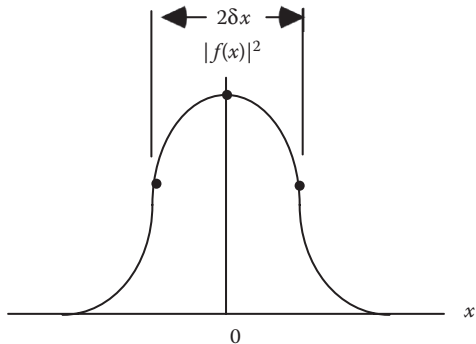


Figure 2.12 A qualitative plot of absolute square of the function, $f(x)$, which results from the Fourier transform of the $g(k)$ function shown in Figure 2.11.

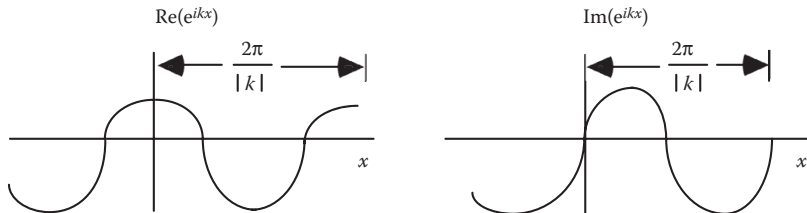


Figure 2.13 The real and imaginary parts of e^{ikx} as a function of x .

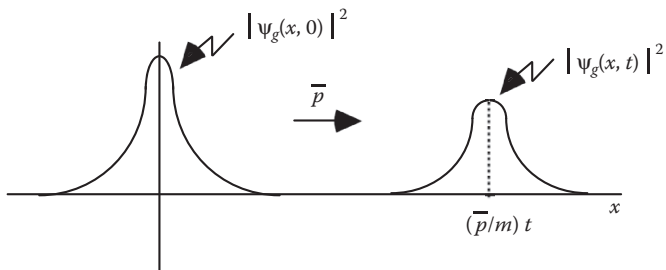


Figure 2.14 Representation of the evolution in time of a Gaussian wave packet.

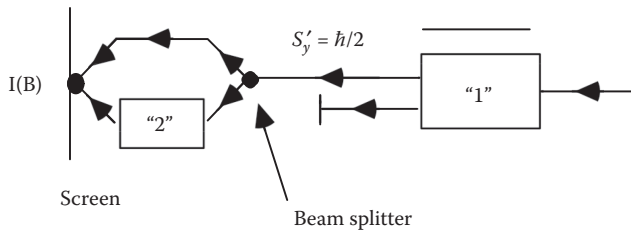


Figure 2.15 A selection/beam-splitting tabletop experiment done with spin 1/2 particles.